Continental Shelf Research 55 (2013) 97–107

Contents lists available at SciVerse ScienceDirect

Continental Shelf Research

journal homepage: www.elsevier.com/locate/csr

Research papers

Circulation on the shelf and the upper slope of the Bay of Biscay

Arnaud Le Boyer [a,*], Guillaume Charria [a], Bernard Le Cann [b], Pascal Lazure [a], Louis Marié [c]

[a] DYNECO-Physed, Ifremer, Centre de Bretagne, BP 70, 29280 Plouzané, France
[b] Laboratoire de Physique des Océans, UMR6523 UBO-CNRS-IRD-IFREMER, Université de Bretagne Occidentale, 6, Avenue Le Gorgeu, Brest, 29238 France
[c] Laboratoire de Physique des Océans, UMR6523 UBO-CNRS-IRD-IFREMER, Ifremer, Centre de Bretagne, BP70, 29280 Plouzané, France

ARTICLE INFO

Article history:
Received 29 June 2012
Received in revised form
10 January 2013
Accepted 11 January 2013
Available online 23 January 2013

Keywords:
Bay of Biscay
Observation
Shelf and slope circulation
Vertical profile
ADCP
Wind driven circulation

ABSTRACT

Here, we used measurements taken with an array of 10 acoustic Doppler current profilers deployed from July 2009 to August 2011 to describe the tidally filtered circulation over the shelf and upper slope on the French side off the French coasts of the Bay of Biscay. The measurements provided an overview of the shelf and slope circulation throughout the entire water column over a large range of spatial and time scales. The average circulation over the shelf and upper slope of the Bay of Biscay was poleward following the topography with a speed of the order of 3 cm s^{-1}. This average circulation had marked seasonal variability. In summer, the currents were equatorward on the outer shelf near surface. Deeper in the water column, the flow remained poleward. In winter, the intensity of the current increased in the north, while it reached its maximum in the south in autumn. On a weekly scale, this behaviour was associated with strong surface currents near the coast in the northern part of the domain in winter and strong currents affected the whole water column in the southern part of the domain in autumn. Correlations of the along-shore currents with wind suggest that wind stress drives almost half of the total observed circulation. We suggest that this forcing acts either directly via local winds or potentially by coastal-trapped waves generated by non-local winds. The potential remote forcing mechanism acts predominately in the southern Bay of Biscay when the wind blows eastward along the northern Spanish coast.

1. Introduction

The continental shelf of the Bay of Biscay (BoB) west of France is located in the eastern part of the Atlantic Ocean between Capbreton Canyon and Penmarc'h Point (Fig. 1). One feature of the BoB is the northward widening of the shelf. From the Spanish coast to Penmarc'h Point, the width of the continental shelf varies from ~60 km to ~160 km in front of the Loire River. This study focuses on the circulation on the shelf and the upper part of the continental slope. The continental slope is irregular and has many promontories and canyons (Fig. 1). The first large-scale studies of the area were hydrological (e.g. Vincent and Kurc, 1969a; Le Cann, 1982, 1988; Puillat et al., 2004). They show a seasonal (from spring to autumn) bottom-trapped water mass with a temperature of 12 °C between the 60 m and 120 m isobaths. This so-called "bourrelet froid" (cold pool) appears after the seasonal thermocline sets up, insulating the bottom water. This type of pattern has been observed in other regions such as the Irish Sea (Brown et al., 2003) and over the Mid-Atlantic Bight (Houghton et al., 1982). The surface temperatures vary from 10 °C in the north in winter to >21 °C in the south in summer. With the exception of winter, the thermocline depth is similar to the depth of the 12 °C isotherm at ~40 m depth in spring and ~70 m depth in autumn. In winter, the water masses are homogeneous in the vertical profile.

Despite its complex topography, this area features a classical eastern boundary current system, with poleward flow on the shelf and slope (Koutsikopoulos and Le Cann, 1996) and is influenced by the eastern edge of the large-scale oceanic basin circulation (Pollard and Pu, 1985). These open ocean boundary conditions force the slope current to be unstable and generate eddies observed in the interior of the BoB. In addition, these conditions can act in concert with the wind and the buoyancy gradient and drive shelf circulation.

The complex circulation of the BoB has been studied for several years with in situ data. Over the abyssal plain, the average circulation shows a very weak (1–2 cm s^{-1}) anticyclonic trend (Pingree, 1993). However, the circulation is affected by mesoscale dynamics. Anticyclonic eddies called SWODDies (Slope Water Oceanic EDDies) (Pingree and Le Cann, 1992) are generated on the slope of the BoB. The generation of these eddies influences the circulation of the open and coastal ocean. The slope current was documented by Pingree and Le Cann (1990) who used available current meter data to establish its flow at a mean speed of

* Corresponding author. Tel.: +33298224330
E-mail address: arnaud.leboyer@ifremer.fr (A. Le Boyer).

0278-4343/$ - see front matter
http://dx.doi.org/10.1016/j.csr.2013.01.006

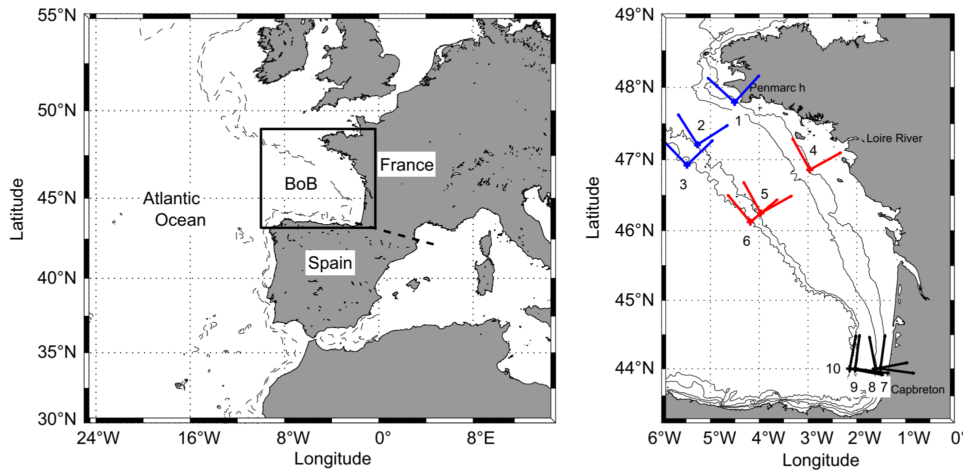

Fig. 1. (a) Location of the Bay of Biscay (BoB) in the North Atlantic Ocean. (b) Mooring positions in the ASPEX project. The numbers refer to the ASPEX mooring nomenclature. Blue: the Penmarc'h section. Red: the Loire River section. Black : the 44°N section. Thin black lines indicate the 60, 100, 130 and 450 m isobaths. The vectors denote the along-shore and cross-shore directions obtained using the empirical orthogonal function method (see text). (For interpretation of the references to color in this figure caption, the reader is referred to the web version of this paper.)

5–10 cm s^{-1}. This current is highly seasonal and geographically influenced. Van Aken (2002) and Charria et al. (2013) used data from drifters collected over the last 17 years to analyse the surface circulation ($\sim$15 to 80 m depth) of the BoB. Given the amount of drifter data, the surface circulation could be accurately described. The data indicate mean poleward circulation on the slope and strong seasonal variability on the shelf. For spring and summer, the surface circulation, on the French side of the BoB shelf and slope (hereafter, BoBSS), is equatorward, while in winter and autumn, at the surface, water masses flow poleward. The circulation in the BoB is strongly influenced by the seasonal variation of wind (Pingree and Le Cann, 1989), heat fluxes (Somavilla et al., 2013) and freshwater inflow (Lazure and Jegou, 1998; Lazure et al., 2008; Ferrer et al., 2009).

To improve our knowledge of the circulation in the BoBSS, the objective of the ASPEX project was to observe the shelf and upper continental slope circulation through the water column over large spatial and temporal ranges. This study focuses on the seasonal dynamics and the horizontal velocities observed over a two-year period, from July 2009 to August 2011. In Section 2, we describe the ASPEX scientific project from which we obtained the current data and the numerical model to explore wind-driven circulation in the BoB. In Section 3, we present a seasonal analysis of the wind regime and the observed circulation in the BoB using different time scales. Then, we discuss in Section 4 the influence of the wind on the observed circulation in the BoB and other mechanisms that also drive the circulation. Finally, we draw conclusions from our study in Section 5.

2. Data and methods

2.1. ASPEX experiment

During the ASPEX project, 10 current-meter moorings were deployed over the shelf and the upper part of the slope of the BoB from July 2009 to August 2011. They were set out in three sections (see Fig. 1). Moorings 1, 2, 3 constituted the "Penmarc'h section". Moorings 4, 5, 6 composed the "Loire section". The last section along 44°N, north of the Capbreton Canyon was called the "44°N section" with moorings 7, 8, 9 and 10.

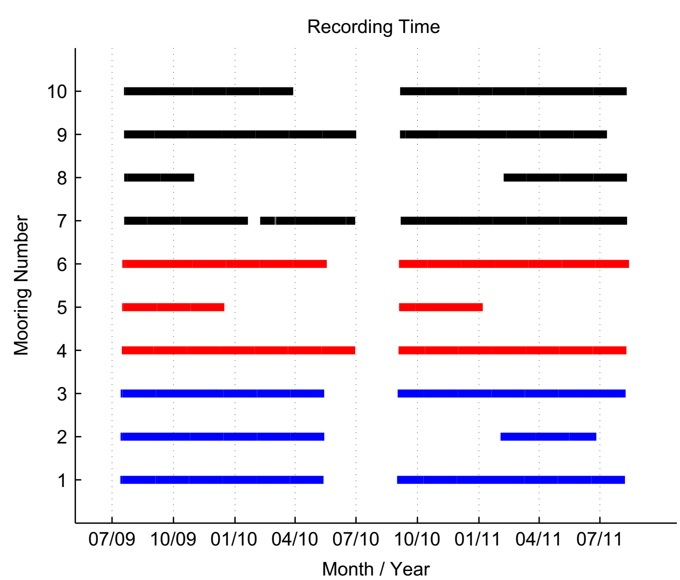

Fig. 2. Length of the time record for each mooring after removing outlier data. The colours blue, red and black represent the Penmarc'h, Loire and 44°N sections. (For interpretation of the references to color in this figure caption, the reader is referred to the web version of this paper.)

Each section was instrumented along three isobaths with RDI WorkHorse acoustic Doppler current profilers (ADCP): $\sim$450 m isobath (moorings 3, 6, 10) with ADCPs operating at 75 kHz, $\sim$130 m isobath (mooring 2, 5, 9) with ADCPs operating at 150 kHz and the $\sim$60 m isobath (moorings 1, 4, 7) with ADCPs operating at 300 kHz. Mooring 8 was an ADCP operating at 300 kHz but deployed on the 70 m isobath. The ADCPs were not deployed exactly on the 450 m, 130 m, 70 m and 60 m isobaths; however, for the sake of simplicity, these isobath designations were used for the description of the results and the discussion. The moorings were all swivel-mounted on a frame together with an SBE37 Microcat T/S/P recorder. One difficulty concerning the organisation of experiments in this area is the dense fishing activity which can lead to ADCP damage. Special care was taken to detect irregularities in the pressure time series during the

Table 1
ASPEX moorings characteristics.

		Penmarc'h			Loire		
	Mooring number	1	2	3	4	5	6
	Latitude (N)	47°48′	47°13′	46°55′	46°52′	46°15′	46°07′
	Longitude (W)	−4°30′	−5°16′	−5°29′	−2°58′	−3°58′	−4°11′
	Cell size (m)	2	8	16	2	8	16
	Sound frequency (kHz)	300	150	75	300	150	75
	Sampling period (s)	30	30	150	30	30	150
2009 2010	**Mooring depth (m)**	71	130	453	52	135	423
	Start	2009/07/13	2009/07/13	2009/07/14	2009/07/15	2009/07/16	2009/07/16
	End	2010/05/13	2010/05/14	2010/05/14	2010/06/29	2009/12/16	2010/05/18
	Duration (days)	303	304	304	349	152	306
2010 2011	**Mooring depth (m)**	71	138	457	47	135	416
	Start	2010/08/31	2011/02/02	2010/09/01	2010/09/02	2010/09/03	2010/09/03
	End	2011/08/07	2011/06/25	2011/08/08	2011/08/09	2011/01/06	2011/08/13
	Duration (days)	341	143	341	341	125	344
		44°N					
	Mooring number	7	8	9	10		
	Latitude (N)	44°00′	44°00′	44°00′	44°00′		
	Longitude(W)	−1°31′	−1°34′	−2°02′	−2°09′		
	Cell size (m)	2	2	8	16		
	Sound frequency (kHz)	300	300	150	75		
	Sampling period (s)	30	30	30	150		
2009 2010	**Mooring depth (m)**	54	71	138	456		
	Start	2009/07/19	2009/07/19	2009/07/18	2009/07/18		
	End	2010/06/29	2009/10/31	2010/07/01	2010/03/29		
	Duration (days)	327	104	347	253		
2010 2011	**Mooring depth (m)**	54	71	134	454		
	Start	2010/09/05	2011/02/06	2010/09/04	2010/09/05		
	End	2011/08/10	2011/08/10	2011/07/11	2011/08/10		
	Duration (days)	338	184	309	339		

recording associated with trawl contact. These sources of error were removed and the data were linearly fitted to fill the gaps in the time series. Fig. 2 presents the recording time for each mooring after removing the outlier data. Missing data involved mainly the Loire section at the 130 m isobath (mooring 5) and the 44°N section at the 70 m isobath (mooring 8).

Table 1 presents the characteristics of the recorded data from the 10 ADCPs located on the shelf and the upper part of the slope of the BoB for the 2009/2010 period and the 2010/2011 period. The mooring depth represents the time average of the pressure recorded by the instruments converted into meters. Depending on the instrumented isobath, the cell size of the observations was 2 m, 8 m or 16 m for the 60, 130 and 450 m isobaths, respectively. The deepest cell that recorded the current was located above the ADCP at a height of about 1.5 times the cell size. The ADCP beam angle was 20° to the vertical. Due to the beam angle, the reflection of sound at the surface contaminates cells close to the surface. Thus, only $\sim 80\%$ (from the deepest cell to the shallowest cell) of the total water column can be sampled. The sampling period was 30 s for both the 300 kHz and 150 kHz ADCPs and 150 s for the 75 kHz ADCPs. The collected data were then averaged over 20 min periods. Our study will focus on the tidally filtered time series of these currents. To perform the tide filtering, we used the Godin tide filter (Godin, 1972). The cut-off period of the Godin filter is 3.9 days.

The tidally filtered currents were projected into separate along-shore and cross-shore components. Based on the hypothesis that the current variability is strongly constrained by the topography, the along- (cross-) shore direction is defined by the direction which maximises (minimises) current variability. Applying the empirical orthogonal function (EOF) method (Björnsson and Venegas, 1997) to the zonal and meridional components of the vertically averaged and tidally filtered currents, we obtained two EOF modes on which current variability can be projected. The eigenvector associated with the first (second) mode maximises (minimises) this variability and defines the along- (cross-) shore direction. Fig. 1 presents the cross-shore and along-shore directions defined by the EOF method. These directions were defined as poleward-positive for the

Table 2
Seasonal time series characteristics per season and per section. Note that there is no data for summer 2010.

		Penmarch	**Loire**	**44**°N
Summer 2009	Start date	07/16/2009	07/19/2009	07/22/2009
	End date	09/30/2009	09/30/2009	09/30/2009
	Length (days)	76	73	70
	Mooring Id	1 2 3	4 5 6	7 8 9 10
Autumn 2009	Start date	10/01/2009	10/01/2009	10/01/2009
	End date	12/31/2009	12/12/2009	12/31/2009
	Length (days)	91	72	91
	Mooring Id	1 2 3	4 5 6	7 9 10
Winter 2010	Start date	01/01/2010	01/01/2010	02/10/2010
	End date	03/31/2010	03/31/2010	03/26/2010
	Length (days)	89	89	43
	Mooring Id	1 2 3	4 6	7 9 10
Spring 2010	Start date	04/01/2010	04/01/2010	04/01/2010
	End date	05/10/2010	05/15/2010	06/26/2010
	Length (days)	39	44	86
	Mooring Id	1 2 3	4 6	7 9
Autumn 2010	Start date	10/01/2010	10/01/2010	10/01/2010
	End date	12/31/2010	12/31/2010	12/31/2010
	Length (days)	91	91	91
	Mooring Id	1 3	4 5 6	7 9 10
Winter 2011	Start date	02/05/2011	01/01/2011	02/09/2011
	End date	03/31/2011	03/31/2011	03/31/2011
	Length (days)	54	89	50
	Mooring Id	1 2 3	4 6	7 8 9 10
Spring 2011	Start date	04/01/2011	04/01/2011	04/01/2011
	End date	06/22/2011	06/30/2011	06/30/2011
	Length (days)	82	90	90
	Mooring Id	1 2 3	4 6	7 8 9 10
Summer 2011	Start date	07/01/2011	07/01/2011	07/01/2011
	End date	08/04/2011	08/06/2011	08/07/2011
	Length (days)	34	36	37
	Mooring Id	1 3	4 6	7 8 10

along-shore component and positive toward the coast for the cross-shore component.

2.2. Current processing for seasonal circulation

Based on the available collected data, we processed the dataset to define the seasonal currents. These currents were averaged over three-month periods: January, February, March for winter; April, May, June for spring; July, August, September for summer and October, November, December for autumn. We only considered continuous time series longer than one month to define a seasonal time average. This month must be shared by at least two moorings along each section to be taken into account. This criterion ensured a consistent analysis of the seasonal circulation in a given section. Table 2 describes the seasonal time series in each section for each available season. From summer 2009 to summer 2011, the shortest and the longest seasonal time series were about 34 days and 91 days, respectively. During the two years of measurements, the four seasons were each sampled twice. Summer 2010 is missing because the instruments were retrieved and re-deployed during that season. Thus, the associated time series were too short to be significant. Only summer 2009 and summer 2011 were analysed.

2.3. ARPEGE winds

To understand the dynamics of the BoB circulation, we compared the ASPEX data with the winds estimated in the BoB over the two years of measurements. The winds are from the ARPEGE atmospheric general circulation model (GCM) from Météo-France (Déqué et al., 1994). The model outputs were sampled every 6 h and its spatial grid had a 0.5° resolution. We used the ARPEGE winds within a window ranging from 43.5°N to 48.5°N and from 1°W to 7°W.

2.4. Time-lagged wind–current correlations

In Section 3.5, the wind-driven circulation was estimated based on the computation of the time-lagged correlation of the along-shore velocities with the local winds projected on axes varying on angles from 0 to 2π. We focused on time lags shorter than 7 days in order to discuss the synoptic time scales and shorter periods. The maximum correlation and the corresponding angle led to an estimation of the wind component for which the variations of the along-shore currents and winds were in phase. We also had access to the time lags associated with these maximum values of correlation. This information is a good proxy for estimating the influence of local winds or other types of forcing.

3. Results

3.1. Wind regimes in the Bay of Biscay

The EOF method implemented on the BoB wind field indicated that the wind field exhibited weak spatial variation at the scale of the analysis. For the studied period, the first EOF mode explained about 77% of the total variability and the spatial structure (eigenvectors) was uniform. Fig. 3a shows the 1st EOF mode of the winds. It indicates that the wind variations were coherent and similar over the whole BoB.

In Fig. 3b, the wind vectors were spatially averaged over the domain adopted for the wind field. We present here the seasonal evolution of this spatial average. The winds in the BoB are expected to be south-eastward in the summer and mainly north-eastward in the winter with transition periods of two months between each phase. The transition periods should occur in September/October and March/April. These changes in wind direction are called the SOMA effect (Pingree et al., 1999). Nevertheless, the data show that the seasonal wind trends had some inter-annual variability. The wind regime in autumn 2009 was strongly north-eastward and then south-eastward in autumn 2010. This season was marked by a Navidad event (Garcia-Soto and Pingree, 2012). This event and its influence are discussed in Section 4. Furthermore, winter 2010 winds were strongly northward. This is due to two important storms that occurred that winter. One of them was the Xynthia storm which caused much damage on the west coast of France.

3.2. Mean circulation

The observed mean circulation (vertically and time-averaged over the available data) from July 2009 to August 2011 (blue

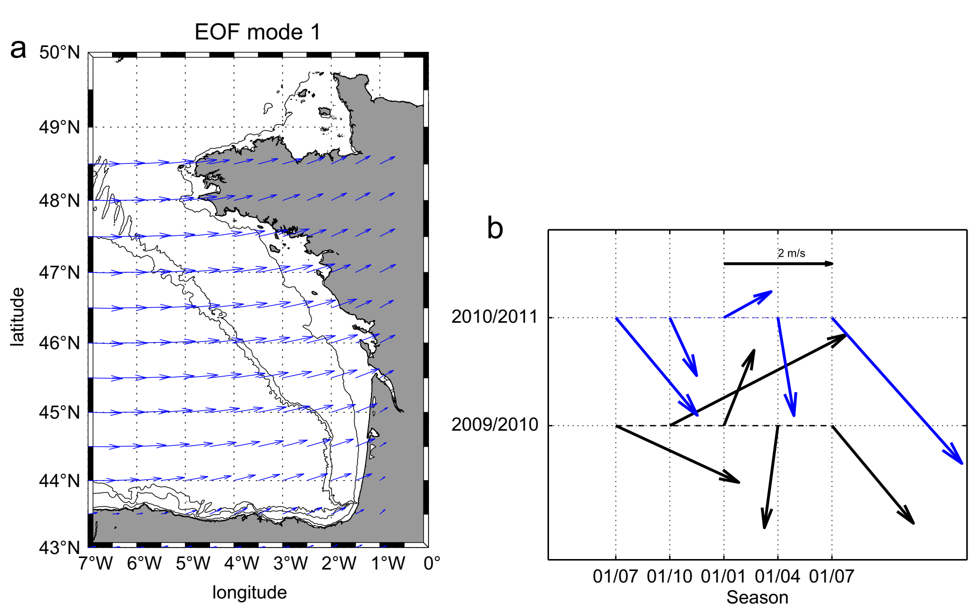

Fig. 3. (a) Spatial structure of the first EOF mode of the Bay of Biscay winds. (b) Monthly averaged wind in the Bay of Biscay for the 2009/2010 period (black) and 2010/2011 period (blue). (For interpretation of the references to color in this figure caption, the reader is referred to the web version of this paper.)

arrows in Fig. 4) is mainly poleward following the topography with currents of the order of 3 cm s^{-1}. On the slope, the mean currents tended to increase poleward, but the circulation on the shelf showed less coherent spatial variability. The strongest mean currents ($\sim$5 cm s^{-1}) were found at the 450 m isobath in the Penmarc'h section and they decreased over the slope to 2 cm s^{-1} in the Loire section and in the 44°N section. The circulation at the mouth of the Loire river was weaker (1 cm s^{-1}) and eastward at the 130 m isobath. In the 44°N section, the mean current at the 60 m isobath was about 4 cm s^{-1}. The results at the 70 m isobath in the 44°N section and at the 130 m isobath at the mouth of the Loire river must be analysed carefully because the associated time series contained less than 200 days (thin arrows in Fig. 4) of data compared to more than 600 days of data for most of the others.

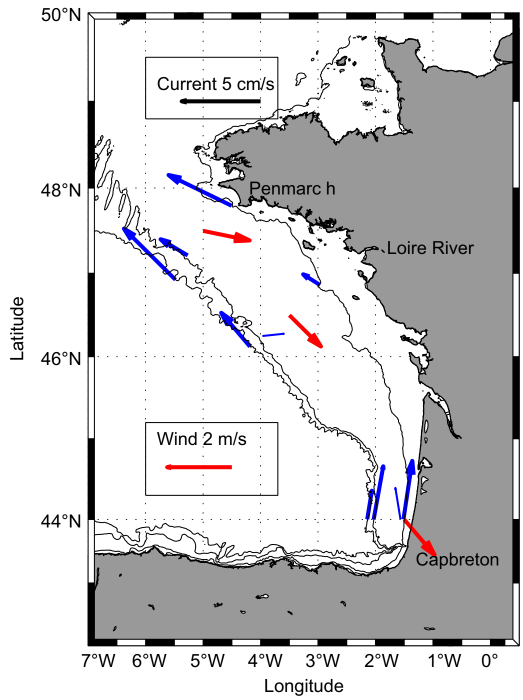

Fig. 4. Two-year average of the vertically averaged currents (blue arrows) and mean winds (red arrows) for the two years of the experiment. The black lines are the 60, 130 and 450 m isobaths. The thin arrows indicate data coverage of less than 200 days. (For interpretation of the references to color in this figure caption, the reader is referred to the web version of this paper.)

These mean currents were compared with the mean winds observed in the middle of each section over the two years of the experiment (Fig. 4, red arrows). The wind at these locations was a good proxy of the wind over the whole section. The mean winds veered southward with decreasing latitudes and the mean currents were poleward following the topography. The mean winds were eastward with an intensity of 2 m s^{-1} along the Penmarc'h latitude and turned southward in the southern part of the BoB. Wind direction opposed current direction in most locations.

3.3. Seasonal circulation

3.3.1. Depth-averaged circulation

The depth-averaged seasonal circulation is shown in Fig. 5a. Similar to the mean circulation over the two years, seasonal currents were generally poleward and they flowed following the topography.

In autumn, the circulation was poleward over the entire BoBSS. Differences appeared in the intensity of the circulation. The intensity of the circulation in the northern part of the BoBSS (Penmarc'h and Loire sections) was similar for currents at the 60 and 450 m isobaths of about 5 cm s^{-1} and weaker currents of about 2 cm s^{-1} at the 130 m isobath. In the 44°N section, the weaker (2 cm s^{-1}) currents were near the coast (60 m isobath). The currents increased offshore with an intensity of about 5 cm s^{-1}.

In winter, the currents were poleward along the 60 m isobaths, increasing northward with a maximum at Penmarc'h about 5 cm s^{-1}. Along the 130 m isobath, the winter currents were poleward and about 3 cm s^{-1} in the Penmarc'h and 44°N sections. The circulation on the upper slope (450 m isobath) in winter was also poleward

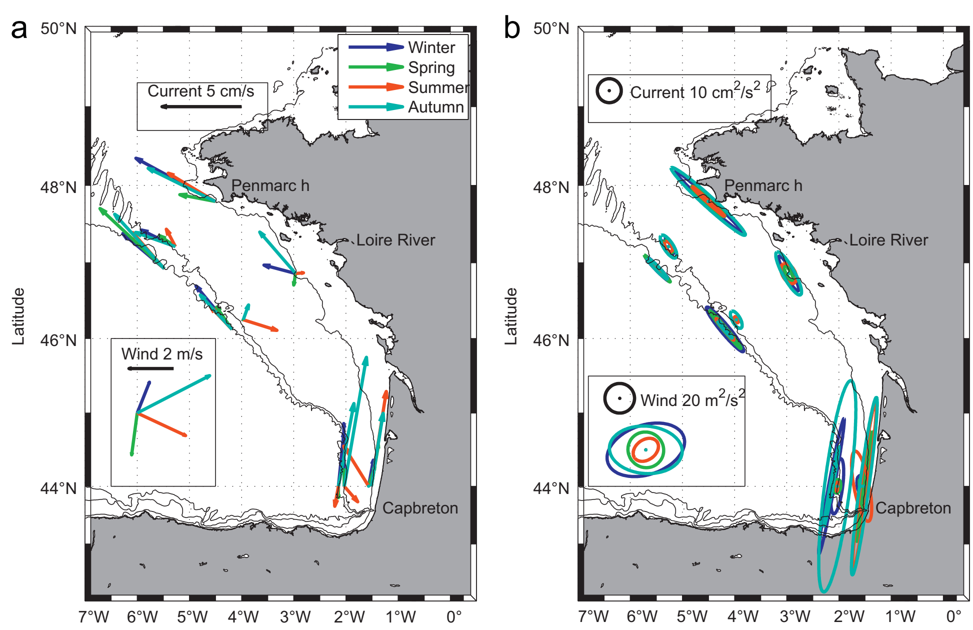

Fig. 5. (a) Seasonal averages of depth-averaged currents. Inset at 45°N–6°W, seasonal and spatial average of the winds over the entire Bay of Biscay. Summer season at all locations and spring in the Penmarc'h section had time series of about one month in one of the two sampled seasons. (b) Seasonal variability of the depth-averaged currents. Inset at 45°N–6°W, seasonal variability of the averaged winds over the entire BoB. Black lines indicate the 60, 130 and 450 m isobaths.

increasing southward with a maximum in the 44°N section about 5 cm s^{-1}.

In spring, the currents were weakly poleward almost everywhere ($\sim$1 cm s^{-1}) in the BoBSS. However, two moorings showed different behaviour. The spring currents in the Penmarc'h section on the upper part of the slope (450 m isobath) were strong (5 cm s^{-1}) and the currents at the 60 m isobath in the Loire section were slightly southward in the same direction as the mean winds over the entire area for spring.

The summer circulation was globally weaker than during winter and autumn. The currents in the Penmarc'h section were poleward with a maximum at the 60 m isobath (5 cm s^{-1}) and a minimum at the 130 m isobath ($\sim$1 cm s^{-1}). In the Loire section, the currents were eastward on the shelf (60 and 130 m isobaths) and poleward on the upper slope (450 m isobath). In the 44°N section, the currents near the coast (60 m isobath) were poleward and the strongest in the area (5 cm s^{-1}). At the 130 m and 450 m isobaths, the currents of the 44°N section were equatorward with an amplitude of $\sim$1 cm s^{-1}.

The seasonal variance of the tidally filtered depth-averaged currents is given in Fig. 5b. Similar to the seasonal averages, the current variability was constrained by the topography with larger variances close to the coast and on the upper slope. The variance in autumn was the greatest along all sections except in the Loire section on the upper slope (450 m isobath) which showed the smallest variance in autumn (10 cm s^{-1}). Current variance amplitude during this season ranged from 6 cm s^{-1} over the 130 m isobath in the Loire section to 100 cm s^{-1} in the 44°N section over the same isobath. In winter, the current variances remained intense with values around 63 cm s^{-1} on the upper slope in the 44°N section or 40 cm s^{-1} above the 60 m isobath in the Penmarc'h section. In spring and summer, current variances were weaker. For example, over the 130 m isobath in the Penmarc'h and 44°N sections, the variance fell to 6 cm s^{-1}.

3.3.2. Seasonal vertical current profiles

Fig. 6 presents the seasonal vertical profiles of the along-shore and cross-shore current components for each section. These

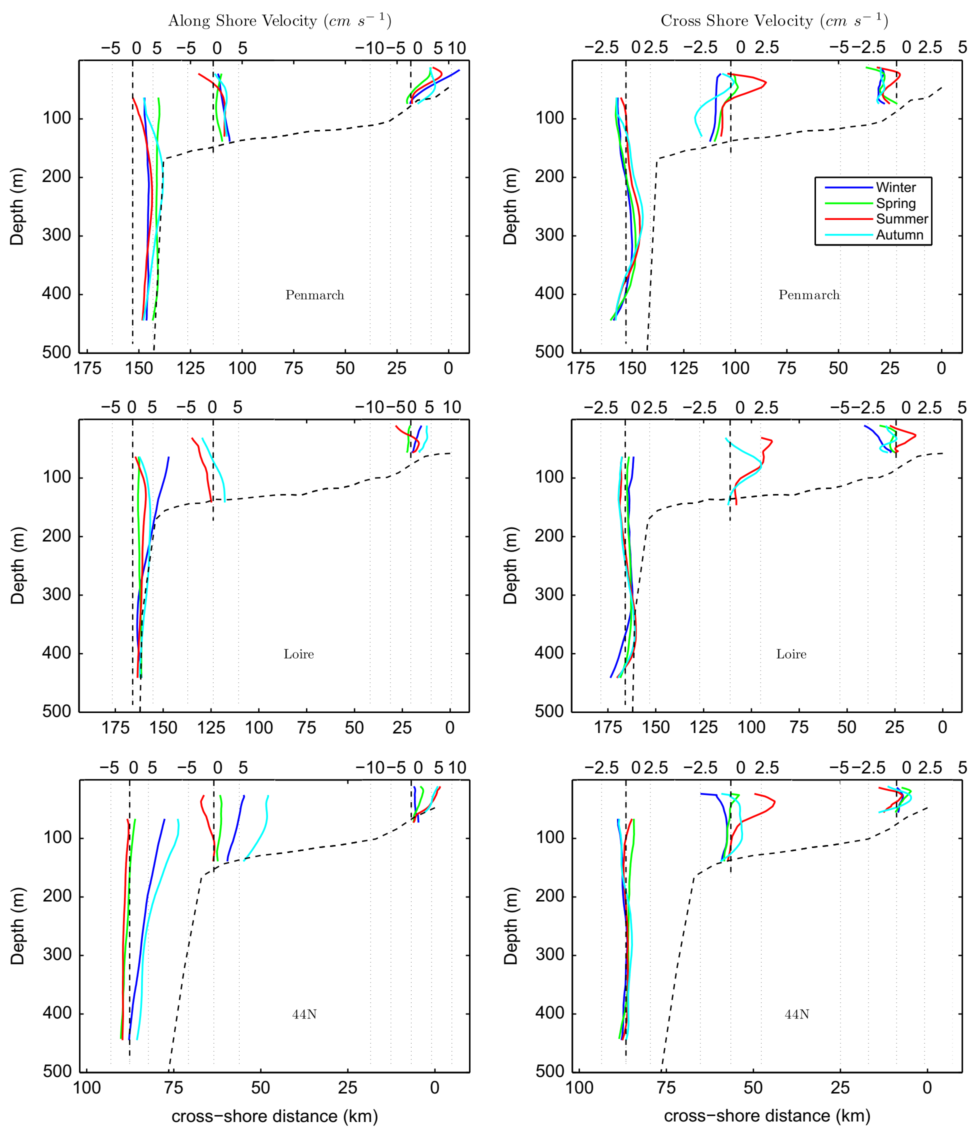

Fig. 6. Seasonal vertical profiles of the along-shore (left panels) positive-poleward and cross-shore (right panels) positive-shoreward components of the currents for Penmarc'h (top panels), Loire (middle panels) and 44°N (bottom panels) sections. Blue lines: winter; green lines: spring; red lines: summer; cyan lines: autumn. *X*-axis scales of the vertical profile are in cm s^{-1} and changes for each isobath. On all these graphs, the position of the profiles was adjusted for the sake of clarity. (For interpretation of the references to color in this figure caption, the reader is referred to the web version of this paper.)

profiles highlight the differences in the shelf and the slope circulations.

Over the 450 m isobath. On the upper slope (450 m isobath), vertical profiles of the along-shore current exhibit poleward circulation except in spring and summer along the 44°N section. However, the vertical structure showed spatial and temporal variability. In winter, Loire and 44°N sections showed increasing velocity from the near-bottom depth (almost null velocity) to the surface (reaching 10 cm s^{-1}). In autumn and summer along the Penmarc'h and Loire sections, the profile had a maximum speed at around 130 m depth (~8 cm s^{-1}). We observed three groups of profiles:

- linearly increasing speed from depth to surface observed during in autumn and winter in the southern part of the BoBSS;
- profiles with maximum poleward speed around 130 m depth in spring and summer in the northern part of the BoBSS;
- profiles with equatorward deep velocities and weak currents at surface in spring and summer in the southern BoBSS.

The vertical profiles of the cross-shore currents were characterised by weaker velocities than in the along-shore direction. The maximum observed cross-shore seasonal mean velocity was ~2 cm s^{-1} in the Penmarc'h section in autumn. We observed downslope velocities near the bottom and upslope velocities above 350–400 m depth with a maximum at 250–350 m depth. The depth of the current inversion slightly changes with the season. Along the 44°N section, the seasonal velocities were weak (1 cm s^{-1}) and showed no important vertical shear and no important seasonal variability.

Over the 130 m isobath. From autumn to spring, currents flowed mainly poleward except in a surface layer along the Loire section (above 70 m depth). However, the shape of the profiles differed between the 44°N and Penmarc'h sections. The largest velocities were observed near the surface in the south and near the bottom in the north (~4 cm s^{-1}). The two sections also differed in seasonal variability, which was strong along the 44°N section with maximum speeds in autumn reaching >10 cm s^{-1}. The summer was the only season when equatorward currents were measured (3 to 5 cm s^{-1} at surface). Along this isobath, cross-shore currents had amplitudes slightly lower than the along-shore current amplitude. In summer, significant upslope currents (~2.5 cm s^{-1}) were observed. The vertical shear, characterised by a subsurface onshore velocity maximum, was also strong along the Penmarc'h and Loire sections and in summer along the 44°N section. On the contrary, in winter, profiles were more vertical and offshore.

Over the 60 m isobath. Along the 60 m isobath, the along-shore currents were mainly poleward reaching 12 cm s^{-1} in the Penmarc'h section in winter at the surface. The mean along-shore velocities were almost nil at the bottom and increased toward the surface. Only the summer profile for the Loire section differed from surface equatorward currents with an intensity of 5 cm s^{-1}.

The vertical profiles of the cross-shore currents at the 60 m isobath were coherent with profiles for the 130 m isobath showing a subsurface maximum trend during spring, summer and autumn. In winter, the vertical profile shape was different. Vertical velocity gradients were weaker suggesting the importance of seasonal stratification for the rest of the year.

3.4. *Weekly circulation*

The amount of energy represented by the variance ellipses and their variability depicted in the previous subsection (Fig. 5) led us to observe results at higher frequencies. The tidally filtered time series of the weekly circulation in the BoBSS at near surface and near bottom depths is given in Fig. 7. The weekly averages of the along-shore currents along the 60, 130 and 450 m isobaths show strong along-shore current values reaching 30 cm s^{-1} close to the surface at all isobaths. The results for the 130 m isobath are not shown because they were similar to the times series at the 450 m isobath with strong currents that occurred for autumn in the southern BoBSS (Fig. 5). Furthermore, at this isobath, the circulation in the two sections (Penmarc'h and Loire) had some gaps in the time series. In the 44°N section, the 450 m isobath showed the strongest along-shore currents. In autumn 2009 and autumn 2010, the current intensity reached >30 cm s^{-1}. These two seasonal events were marked by several monthly episodes of intensified poleward currents. The near-bottom cross-shore currents at this location were always downslope and increased during strong poleward currents (not shown). The strongest currents (>20 cm s^{-1}) along 60 m isobath were at Penmarc'h in spring 2010 and 2011 and in the 44°N section in autumn 2009 and 2010. At the Penmarc'h section, the currents were surface-intensified and at the 44°N section the strong currents were also

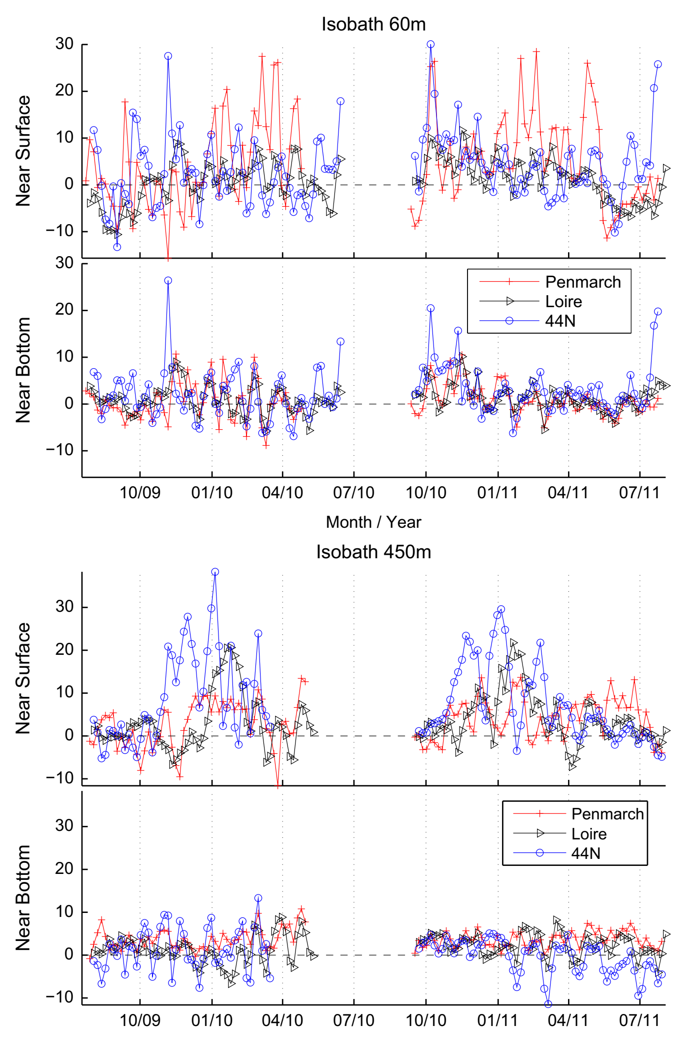

Fig. 7. Weekly average of the along-shore velocities in cm s^{-1} near the bottom and near the surface. Upper and lower panels present the velocities at the 60 m isobath (surface: 7 m depth and bottom: 53 m depth) and the 450 m isobaths (surface: 53 m depth and bottom: 378 m depth), respectively. Red, black and blue lines are velocities at moorings along Penmarc'h, Loire and 44°N sections, respectively. (For interpretation of the references to color in this figure caption, the reader is referred to the web version of this paper.)

observed near the bottom. These strong current events occurring in the 44°N section, either at the 60 m isobath or the 450 m isobath (blue lines), were followed by a current peak in the Loire section (black lines). They occurred in autumn (6 November 2009 at the 60 m isobath and ~ 15 November 2010 at the 450 m isobath) or early winter (~ 1 January 2011 at the 450 m isobath).

The summer and autumn 2009 near-bottom circulation recorded in the 44°N section at the 60 m isobath was not correlated with that observed in the Penmarc'h section. After the barotropic events occurring in the 44°N section, Fig. 7 shows some coherent variations of about 10 cm s^{-1} for the three sections from January to May 2010 with a period of about a month along the 60 m isobath. These coherent oscillations seem to cease at the beginning of summer. This specific behaviour also occurred after autumn 2010 and during winter 2011. At the 450 m isobath, the near-bottom circulation also showed seasonal changes in behaviour. The near-bottom currents were of the order of ±5 cm s^{-1} for summer and autumn in both years (2009 and 2010) while they stayed of the order of ±10 cm s^{-1} for the rest of the year (winter and spring). Oscillations observed near the bottom such as the ones observed on the 60 m isobath occurred only in the southern BoB for late autumn 2009, winter 2010, winter and spring 2011. In the Penmarc'h and Loire sections, the variability of the along-shore current along the 450 m isobath fell within a range of −1 cm s^{-1} to 10 cm s^{-1}. The 450 m isobath circulations in these sections for stratified seasons (summer and autumn) occurred during the same period of time while for winter and spring, the Loire section currents were similar to the 44°N section current variations.

Coherent flows all over the BoB or over a large part of the area may be the response to large-scale forcing. In Section 4, we discuss the possibility that large-scale forcing is responsible for the circulation [patterns] observed in the BoB.

3.5. Wind driven circulation

The first step toward understanding the tidally filtered BoB circulation is to estimate the wind-driven circulation component from the total circulation. Fig. 8 presents the maximum values of the time-lagged correlations of the depth-averaged along-shore velocities and the local along-shore wind stress along the 60 m isobath. This analysis focuses on the seasonal behaviour of the correlations between the wind stress and depth-averaged along-shore currents.. The correlations are presented as a function of the direction of the wind component that led to these values. Correlation values fell within a range of ~0.4 to 0.8. The correlations of the wind with currents at the 130 m and 450 m isobaths were less than 0.5 (not shown).

The correlations observed at the 60 m isobath can be split into two groups. Some points were located close to the along-shore directions showing that wind in the along-shore direction had a maximal effect and the other group of points was located to the west of these along-shore directions. These two groups can be better characterised according to geographical criterion rather than seasonal influence. For instance, the depth-averaged along-shore currents in the Penmarc'h and Loire sections were correlated with winds projected on the local along-shore directions, whereas in the 44°N section the along shore currents were well correlated with westerlies. In the Loire section, the highest correlation was observed in spring, whereas autumn winds were well correlated with the depth-averaged circulation in the Penmarc'h section. In both sections, correlations decreased slightly in summer. In the 44°N section, only the correlation in winter 2010 (blue triangles) aligned with the local along-shore direction (i.e. north–south). None of other seasonal along-shore current–wind correlations in this section were aligned with the along-shore direction and the associated points were thus part of the second group of points that we defined. Some other correlation points did not align with the local topography in the Penmarc'h section for winter 2010 and Loire section for summer 2009, winter 2010 and autumn 2010. Thus, correlations were not influenced by local winds and may indicate a remote forcing mechanism transmitted by coastal-trapped waves.

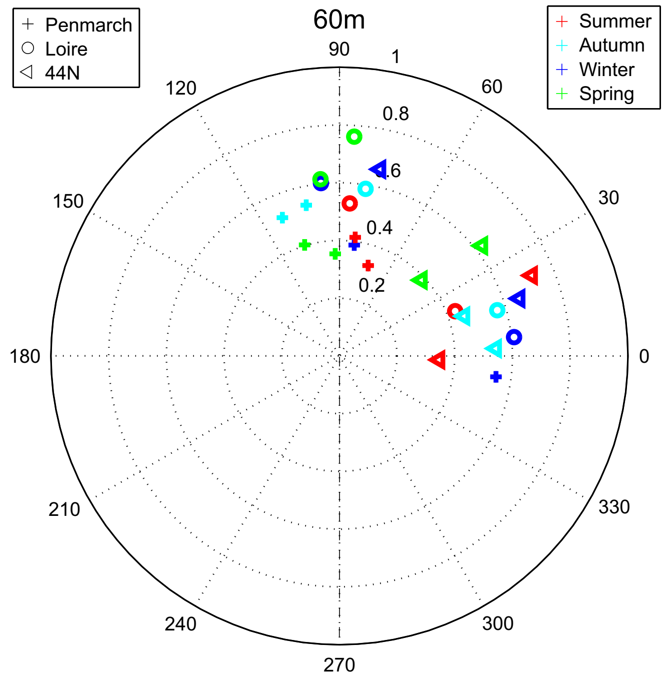

Fig. 8. Maximum correlations of the depth-averaged alongshore velocities at the 60 m isobath with local wind. The radii give the value of the correlation, the azimuths give the wind orientation relative to the poleward along-shore circulation where the maximum correlation was reached. The crosses, circles and triangles are the Penmarc'h, Loire and 44°N section's moorings, respectively. The red, cyan, blue and green symbols represent the summer, autumn, winter and spring seasons, respectively. The black dashed lines represent the local along-shore direction of the 60 m isobath in the Penmarc'h, Loire and 44°N sections. (For interpretation of the references to color in this figure caption, the reader is referred to the web version of this paper.)

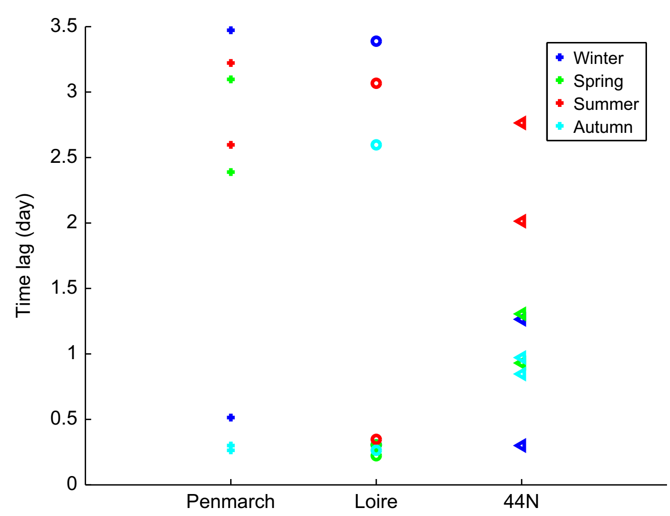

Fig. 9. Time lags (in days) that give the maximum correlation values presented in Fig. 8. The time lags are presented per section and per season: winter in blue; spring in green; summer in red and autumn in cyan. (For interpretation of the references to color in this figure caption, the reader is referred to the web version of this paper.)

Fig. 9 gives the time lags in days that produced the maximum correlations presented in Fig. 8. The maximum correlation was obtained for time lags varying from 0 to 3.5 days. The Penmarc'h and Loire sections showed either time lags of ~ 10 h or longer time lags from 2.5 to 3.5 days. In the 44°N section, the time lags were about 1 day. In summer, time lags increased to 2–3 days and only winter 2010 showed time lags of 10 h. Most of the correlation points that were aligned with the local along-shore direction had time lags shorter than 10 h.

4. Discussion

4.1. Bay of Biscay circulation

4.1.1. Mean circulation

The BoB area is characterised by mean wind veering from eastward to south-eastward following the edge of the Azores anticyclone (Fig. 4) (Isemer and Hasse, 1987). Through Ekman transport, the mean wind regime would tend to drive southward to south-westward flow. However, the tidally filtered circulation on the BoBSS was characterised by a mean poleward current. It is interesting to compare the circulation in the BoB to the one over the Mid-Atlantic Bight (MAB) for four reasons. First, they are both complex in configuration with presence of canyons and promontories; second, they are both located at mid-latitudes; third, the tidal currents are comparable; finally, their stratification is influenced by both freshwater runoff and summer heat fluxes. Furthermore, in the MAB, the winds are also perpendicular to the coast (Lentz, 2008) and the mean flow is oriented in a direction that leaves shallow waters on the right. Different forcing mechanisms underlying the mean circulation have been proposed. The runoff of freshwater from rivers, upwelling dynamics or frontogenesis can force a cross-shelf density gradient and contribute to forcing an along-shore current (Csanady, 1978; Beardsley and Winant, 1979). On the other hand, shelf circulation is viewed as a boundary layer of the open ocean, thus indirectly driven by large-scale wind stress and heat fluxes that lead to an along-shore pressure gradient (Csanady, 1978). This study shows that shelf circulation is most likely a response to the boundary conditions set up by the open ocean and the coastal circulation that occurs north of the MAB (Chapman and Beardsley, 1989). However, Lentz (2008) recently showed that the buoyancy-driven flow in equilibrium with the cross-shelf density gradient can be described by observations after simply removing the wind-driven circulation. Thus, the shelf and upper slope tidally filtered circulation may be the combination of large-scale and local forcing. The simultaneous influence of different forcing scales adds complexity to studying shelf and slope circulations. Our study corroborates this complex interaction of forcing with the observation of two different dynamics on the upper slope and the shelf (see Fig. 7), but the separate influence of both types of forcing needs to be analysed more carefully to confirm this interaction of different scales of forcing.

The influence of a possible large-scale forcing was studied by Pingree and Le Cann (1989). Through numerical experiments, they obtained patterns of circulation on the slope and the northern part of BoB shelf with the same current intensity and orientation as our observations. They explained this vertically averaged poleward circulation on the slope as a result of the combination of the large-scale meridional density gradient and the steep slope known as the JEBAR term (Huthnance, 1984). On the northern part of the French continental slope, Pingree and Le Cann (1989) found current intensity associated with this term comparable to the circulation observed here (~ 5 cm s^{-1}). The shelf residual circulation observed in Pingree et al. was also poleward but the slope was not steep enough to drive a JEBAR current comparable to our observations. The cross-shelf density gradient, as a consequence of the freshwater runoff from French rivers (Lazure and Jegou, 1998), can also drive this poleward current, but these runoffs are strongly seasonal. In the next subsection, we will discuss the influence of wind forcing on shelf circulation.

4.1.2. Seasonal circulation

The seasonal averages show a relatively weak circulation over the upper slope and shelf of the BoB and important seasonal and geographical variability (Fig. 7). In winter, our results show tidally filtered current intensities of up to about 40 cm s^{-1} at the surface of the Penmarc'h section at the 60 m isobath while, in the 44°N section, strong currents occurred in summer and autumn with a deep vertical extension. With the exception of these short, strong current events in the 44°N section on each of the instrumented isobaths, the near-bottom circulation on the shelf of the BoB showed coherent flows over a large spatial scale. Current oscillations occurred in late winter and spring with period of one month. For the rest of the year, the currents in the Loire section were correlated either with the 44°N section circulation or the Penmarc'h section circulation. This suggests wind forcing over the same large spatial scale. In Section 4.2, we demonstrated the influence of either local or remote winds on this circulation.

The ASPEX data complements the near-surface drifter data organised and described in Charria et al. (2013). Looking deeper in the water column, the main seasonal patterns of the surface circulation were similar: strong and poleward autumnal currents, weak shelf circulation in spring and equatorward currents in summer. However, some differences appeared in winter where the currents recorded by the ADCP were strong and poleward over the entire shelf although the lack of information from drifters in the northern part of the BoB led to an underestimation of the circulation in this area. Due to the typically low stratification in winter, weak differences between the surface circulation and the interior flow are expected. Thus, the weak circulation observed by drifters can be explained by fewer drifter data in winter or inter-annual variability in BoB circulation. The winter circulation of the BoBSS is frequently marked by a large-scale poleward current off northern Spain (called "Navidad", Pingree, 1994). Garcia-Soto and Pingree (2012) observed several marked Navidad events over the last three decades (1979–2010), all along northern Spain, with an irregular periodicity of 2–6 years (mean, 3 years; standard deviation, ~ 1 year). The most recent Navidad event occurred in late 2009 during the ASPEX project. This event most likely influenced the strong and barotropic current event observed in the southern part of the BoBSS during the autumn season.

Our study also highlights the seasonality of the shelf circulation, especially the seasonal differences between summer circulation and that of the rest of the year. For the summer season, the mean vertically averaged currents presented equatorward currents on the shelf in front of the Loire River and close to the shelf break in the southern part of the BoB (see Fig. 5). Along the 130 m isobath in the Loire and 44°N sections, these equatorward currents increased from the bottom to the surface. At the 60 m isobath in front of the Loire river, we observed a marked vertical shear with equatorward currents at the surface and poleward currents at the bottom (see Fig. 6). For this season, the south-eastward wind regime can drive surface-intensified equatorward flow but, it does not drive the entire deep circulation in the middle of the continental shelf in front of the Loire River. At this location, Vincent and Kurc (1969b) described a structure called a "bourrelet froid" (cold pool) which appears after the seasonal thermocline sets up. This structure tends to drive a surface-intensified cyclonic circulation in front of the Loire

River (i.e. poleward flow close to the coast) in the interior of the water column (Charria et al., 2013). This kind of cyclonic circulation around a cold pool has been observed in the Celtic and Irish Seas (Hill, 1993).

Another feature of summer circulation is the shape of the vertical profiles of the cross-shore velocity component (Fig. 6). On the shelf, we observed a weak or slightly offshore flow at the bottom, whereas there was a markedly onshore current at the depth of the thermocline. This pattern has been observed along the western American coast (Lentz and Trowbridge, 2001) and over the MAB (Lentz, 2008). Furthermore, it fits with the theoretical framework of the arrested topographic wave (ATW) (Csanady, 1978). An along-shore jet with shallow water on the right can drive a downslope current at the bottom in the Ekman layer. By continuity, it leads to an onslope interior flow. However, this type of pattern observed with an ADCP has to be analysed carefully because, in a region with enhanced internal wave activities (Pingree and New, 1989), the recorded time series may have strong biases at the thermocline depth. An ADCP records current velocities at fixed depths; thus, the velocities in the layers above and below the thermocline are recorded by the same cell due to the vertical displacement of the thermocline that arises from the presence of internal waves (Pingree and Le Cann, 1989). From the shelf break to the coast, this may lead to an increase in the observed mean cross-shore velocity in the direction of the phase speed propagation of the internal wave, because the velocity fields of internal waves above and below the thermocline are opposed (Phillips, 1977). This observed feature on the vertical profiles of the cross-shore currents (Fig. 6) can be forced either by the ATW mechanism or through biases in Eulerian measurements of an internal wave field.

An internal wave field can also influence circulation at the 450 m isobath. This isobath was approximately the depth where internal waves are generated through interaction with topography. Internal wave beams are generated at the shelf break and propagate downslope at an angle with the slope depending on the stratification at the location where it is generated. These waves have strong spatial variability and the mean currents associated with these waves can reach ~ 15 cm s^{-1} on the upper slope near "La Chapelle" bank in the north of the BoBSS (Pingree and Le Cann, 1989).

4.2. Wind driven circulation

The correlations between local winds and along-shore velocities (>0.5) suggest that the wind has a strong influence on the circulation at the 60 m isobath. However, our results (see Figs. 8 and 9) suggest two kinds of processes that occur on the BoBSS. The oriented time-lagged correlations can be divided into two groups based on wind direction and time-lag criteria. On the one hand, the observed along-shore circulation was well correlated with the along-shore wind and the time-lags associated with this dynamic were approximately 12 h. Depth-averaged dynamics are primarily forced by wind stress, along-shelf pressure gradients, and bottom stress (Lentz and Fewings, 2012). A simple frictional and barotropic model (Csanady, 1982) assumes a time-scale adjustment to wind forcing defined by $T=H/r$, where T is the time-scale adjustment, H is the water column height and r the linear bottom friction. In the BoBSS, r is approximated as $r=C_d|u_{tide}|$ with $C_d=2.5\times10^{-3}$ a friction coefficient and $|u_{tide}|=0.5$ m s^{-1} an approximation of the tide current intensity. At the 60 m isobath and for a linear bottom friction $r=1.3\times10^{-3}$ m s^{-1}, we obtain a time-scale adjustment of 12 h. This value is comparable to the time-lags we observed in the BoBSS. On the other hand, at 44°N, the observed along-shore circulation was well-correlated with westerlies and the time-lags associated with this dynamics are longer than a day. This suggests local along-shore currents forced by remote winds. This type of mechanism implies a longer time-lag (Lentz and Fewings, 2012) than that necessary for a mechanism whereby along-shore currents are driven by the local along-shore winds. Batifoulier et al. (2012) described the circulation in the southern part of the BoB as influenced by the northern Spanish coast circulation in summer and autumn. For these seasons, stratification is pronounced and the westerlies drive downwelling circulation. The adjustment of the thermocline to the wind generates baroclinic waves associated with strong current events. In our study, ASPEX data suggest that the southern part of the BoB is influenced by the northern Spanish coast circulation during the whole year.

Some correlation points in the Penmarc'h section do not fit with either the frictional model or the remote wind forcing explanation. For spring and summer in this section, the correlation points were aligned with the local along-shore direction with values of 0.4 and time-lags of about 2–3 days. This indicates a weak driving influence of the along-shore winds on the local circulation. This also strongly suggests that some other mechanisms are able to force the main part of the circulation in this section. These other mechanisms may be the driving mechanisms of the $\sim 40\%$ of the observed circulation which could not be explained by wind forcing in the other sections.

5. Conclusion

The circulation in the BoB was estimated at 10 locations with observations throughout the water column from the coast to the upper slope at the 60 m, 130 m and 450 m isobaths along three sections. The nearly two-year time series was used to describe the mean circulation and its temporal evolution as circulation along an eastern ocean boundary. We demonstrated that depth and seasonally averaged currents are poleward throughout the BoB except in summer on the shelf in front of the Loire River where the currents can be equatorward. The seasonal variability of these currents is constrained by the topography and is weaker on the 130 m isobath. On the slope, the cross-shore currents are slightly downslope from mid-depth to the near bottom. On the shelf, the near-bottom flow is also offshore, but in the interior, the vertical profiles show greater variability likely due to wind, the cross-shore gradient density and some bias due to Eulerian measurements of internal wave activity. The temporal evolution of the circulation shows strong barotropic events observed at 60 m depth during summer and autumn in the southern BoB. During the winter season, the circulation in the north is characterised by a strong surface intensified variability, and, close to the bottom, oscillations of the weekly averaged current can be observed throughout the Bay of Biscay shelf and slope.

The BoBSS circulation may be mainly driven by large-scale along-shore pressure gradients, cross-shore buoyancy gradients and local winds. The data from the ASPEX experiment provided good proxies to separate each of these forcing mechanisms. Here, as a first approach, we estimated wind-driven circulation. At the coast, wind-driven circulation appears to be about 60% of the total circulation. Locally, in the Penmarc'h and Loire River sections, the variability of the along-shore currents is driven by the along-shore winds with a spin-up time of around 10 h. In the 44°N section, the circulation is likely indirectly driven by the wind blowing along the Spanish coast. Here, the influence of the wind is time-lagged because the currents are possibly remotely forced through coastal-trapped wave propagation. The repetition of strong current events from year to year indicates that the circulation in the French part of the BoBSS is consistent in time despite changes in atmospheric forcing and/or the presence or absence of the Navidad current.

Acknowledgements

This work is part of the EPIGRAM project supported by the Agence Nationale de la Recherche [French National Research Agency] (Grant ANR-08-BLAN-0330-01) and CNRS/INSU national programme LEFE/IDAO. Special thanks to the institutes that provided the data for this study: IFREMER, Météo-France. The authors would also like to thank the technical staff who worked on the preparation, deployment and the recovery of the instruments.

Appendix A. Wind stress

There are many formulae for computing wind stress (Geernaert, 1987). For this study, we used the wind stress formula from Smith and Banke (1975)

$$Cs = 0.63 + 0.066|\overrightarrow{u_{10}}| \tag{A.1a}$$

$$\overrightarrow{\tau} = \rho_a Cs|\overrightarrow{u_{10}}|\overrightarrow{u_{10}} \tag{A.1b}$$

$\overrightarrow{u_{10}}$ is the wind vector measured at 10 m above the sea level, ρ_a is the air density ($\rho_a = 1.2$ kg m^{-3}) and C_s the drag coefficient.

References

Batifoulier, F., Lazure, P., Bonneton, P., 2012. Poleward coastal jets induced by westerlies in the Bay of Biscay. Journal of Geophysical Research 117 (C3), 1–19.

Beardsley, R., Winant, C., 1979. On the mean circulation in the Mid-Atlantic Bight. Journal of Physical Oceanography 9, 612–619.

Björnsson, H., Venegas, S., 1997. A manual for EOF and SVD analyses of climate data. Report. No 97-1, Department of Atmospheric and Oceanic Sciences and Centre for Climate and Global Change Research, McGill University, p. 52.

Brown, J., Carrillo, L., Fernand, L., Horsburgh, K., Hill, A.E., Young, E., Medler, K., 2003. Observations of the physical structure and seasonal jet-like circulation of the Celtic Sea and St. George's Channel of the Irish Sea. Continental Shelf Research 23 (6), 533–561.

Chapman, D.C., Beardsley, R., 1989. On the origin of Shelf water in the Middle Atlantic Bight. Journal of Physical Oceanography 3, 384–391.

Charria, G., Lazure, P., Le Cann, B., Serpette, A., Reverdin, G., Louazel, S., Batifoulier, F., Dumas, F., Pichon, A., Morel, Y., 2013. Surface layer circulation derived from Lagrangian drifters in the Bay of Biscay. Journal of Marine Systems 109-110, S60-S76, http://dx.doi.org/10.1016/j.jmarsys2012.09.015.

Csanady, G.T., 1978. The arrested topographic wave. Journal of Physical Oceanography 8, 47–62.

Csanady, G.T., 1982. Circulation in the Coastal Ocean, vol. 2687. Springer's Edition. D. Reidel Publishing Company.

Déqué, M., Dreveton, C., Braun, A., Cariolle, D., 1994. The ARPEGE/IFS atmosphere model: a contribution to the French community climate modelling. Climate Dynamics 5555, 249–266.

Ferrer, L., Fontán, A., Mader, J., Chust, G., González, M., Valencia, V., Uriarte, A., Collins, M., 2009. Low-salinity plumes in the oceanic region of the Basque Country. Continental Shelf Research 29 (Apr. (8)), 970–984.

Garcia-Soto, C., Pingree, R.D., 2012. Atlantic multidecadal oscillation (AMO) and sea surface temperature in the Bay of Biscay and adjacent regions. Journal of the Marine Biological Association of the United Kingdom 92 (2), 213–234.

Geernaert, G., 1987. On the importance of the drag coefficient in air–sea interactions. Dynamics of Atmospheres and Oceans 11, 19–38.

Godin, G., 1972. The Analysis of Tide. University of Toronto, Press. (264 pp).

Hill, A.E., 1993. Seasonal gyres in shelf seas. Annales Geophysicae-Atmosphere Hydrospheres and Space 11 (11–12), 1130–1137.

Houghton, R., Schlitz, R., Beardsley, R., Butman, B., Chamberlin, J., 1982. Middle Atlantic Bight cold pool: evolution of the temperature structure during summer 1979. Journal of Physical Oceanography 12 (10), 1019–1029.

Huthnance, J.M., 1984. Slope currents and "JEBAR". Journal of Physical Oceanography 14, 795–810.

Isemer, H., Hasse, L., 1987. The Bunker Climate atlas of the North Atlantic Ocean. Volume II: Air–Sea Interactions. Springer-v Edition. vol. II.

Koutsikopoulos, C., Le Cann, B., 1996. Physical processes and hydrological structures related to the Bay of Biscay anchovy. Scientia Marina 60, 9–19.

Lazure, P., Dumas, F., Vrignaud, C., 2008. Circulation on the Armorican shelf (Bay of Biscay) in autumn. Journal of Marine Systems 72 (Jul. (1–4)), 218–237.

Lazure, P., Jegou, A.M., 1998. 3D modelling of seasonal evolution of Loire and Gironde plumes on Biscay Bay continental shelf. Oceanologica Acta 21 (2), 165–177.

Le Cann, B., 1982. Evolution annuelle de la structure hydrologique du Plateau Continental au sud de la Bretagne. Ph.D. Thesis, Université de Bretagne Occidentale.

Le Cann, B., 1988. Dépouillement des données de courants, de températures et d'hydrologie (03/03/198724/04/1987), CIRESOL. Technical Report, Université de Bretagne Occidentale.

Lentz, S., Trowbridge, J., 2001. A dynamical description of fall and winter mean current profiles over the northern California Shelf. Journal of Physical Oceanography 31 (4), 914–931.

Lentz, S.J., 2008. Seasonal variations in the circulation over the middle Atlantic bight Continental shelf. Journal of Physical Oceanography 38 (Jul.(7)), 1486–1500.

Lentz, S.J., Fewings, M.R., 2012. The wind- and wave-driven inner-shelf circulation. Annual Review of Marine Science 4 (1), 317–343.

Phillips, O.M., 1977. The Dynamics of the Upper Ocean. Cambridge University Press, London.

Pingree, R., Sinha, B., Griffiths, C.R., 1999. Seasonality of the European slope current (Goban Spur) and ocean margin exchange. Continental Shelf Research 19 (7), 929–975.

Pingree, R., 1994. Winter Warming in the southern Bay of Biscay and Lagrangian eddy kinematics from a deep drogued ARGOS buoy. Journal of the Marine Biological Association of the United Kingdom 74, 107–128.

Pingree, R., 1993. Flow of surface waters to the west of the British Isles and in the Bay of Biscay. Deep Sea Research Part II: Topical Studies in Oceanography 40 (1–2), 369–388.

Pingree, R., Le Cann, B., 1989. Celtic and Armorican slope and shelf residual currents. Progress in Oceanography 23 (4), 303–338.

Pingree, R.D., Le Cann, B., 1990. Structure, strength and seasonality of the slope currents in the Bay of Biscay region. Journal of the Marine Biological Association of the United Kingdom 70 (04), 857–885.

Pingree, R.D., Le Cann, B., 1992. Three anticyclonic Slope Water Oceanic eDDIES (SWODDIES) in the Southern Bay of Biscay in 1990. Deep-Sea Research 39 (718), 1147–1175.

Pingree, R.D., New, A.L., 1989. Downward propagation of internal tidal energy into the Bay of Biscay. Deep Sea Research Part A. Oceanographic Research Papers 36 (5), 735–758.

Pollard, R., Pu, S., 1985. Structure and circulation of the Upper Atlantic Ocean Northeast of the Azores. Progress in Oceanography 14, 443–462.

Puillat, I., Lazure, P., Jégou, A., Lampert, L., Miller, P., 2004. Hydrographical variability on the French continental shelf in the Bay of Biscay, during the 1990s. Continental Shelf Research 24 (10), 1143–1163.

Smith, S.D., Banke, E.G., 1975. Variation of the sea surface drag coefficient with wind speed. Quarterly Journal of the Royal Meteorological Society 101 (429), 665–673.

Somavilla, R., González-Pola, C., Lavín, A., Rodriguez, C., 2013. Temperature and salinity variability in the south-eastern corner of the Bay of Biscay (NE Atlantic). Journal of Marine Systems 109-110, S105-S120, http://dx.doi.org/10.1016/j.jmarsys.2012.02.010.

Van Aken, H.M., 2002. Surface currents in the Bay of Biscay as observed with drifters between 1995 and 1999. Deep-Sea Research 49, 1071–1086.

Vincent, A., Kurc, G., 1969a. Les Variations de la Situation Thermique dans le Golfe de Gascogne et leur incidence sur l'écologie et la pêche de la sardine en 1968. Revue des Travaux de l'Institut des Pêches maritimes 33 (2), 203–212.

Vincent, A., Kurc, G., 1969b. Variations Saisonnières de la Situation Thermique du Golfe de Gascogne en 1967. Revue des Travaux de l'Institut des Pêches maritimes 33 (1), 79–96.